DOI 10.1007/s00419-004-0343-6

Scaling impacted structures

R. E. Oshiro, M. Alves

Summary The problem of non-scalability of structures under impact loads caused by strain-rate effects is solved in this article by properly correcting the impact velocity. The technique relies on the use of an alternative dimensionless basis, together with a mathematical model which allows the calculation of a correction factor for the impact velocity. This new velocity, when applied to the model, makes it to assure the satisfaction of the scaling laws. The indirect similitude method detailed here is applied to two strain-rate sensitive structures, a double plate under in-plane impact and a beam subjected to a blast load. The results show a very good agreement so that the model and a prototype made from strain rate sensitive materials behave the same.

Keywords Impact, Similarity, Scaling, Strain-rate effect

1
Introduction

Structures subjected to severe dynamic loads present many features whose understanding and analysis can be rather troublesome. Inertia effects, material response due to strain-rate effects and thermal loading, material failure and stability are a few topics which have been attracting the attention of many researchers. Despite substantial advances in theoretical and numerical models, it is not accepted as yet by regulating authorities the certification of sophisticated structures, e.g. airplanes, without full-scale experimental tests. Full-scale tests can obviously be quite expensive and time consuming, demanding for special rigs and instrumentation. Clearly, the number of these tests can be drastically reduced as numerical and theoretical models advance. They can also be reduced in number and cost by performing tests in scaled models, i.e. in structures whose dimensions have been increased or decreased in concerto by a single factor.

Scaled models can be very attractive when considering the dimensions of structures like trains, ships and airplanes. Testing a scaled airplane to impact loads, for instance, is much more practical than a full scale test. Of course, that if scaled models are to be used, care must be exercised in order to ensure that the so-called scaling laws are valid for the structure under analysis. They were developed in the past on a strong theoretical basis and an overview of them applied to impacted structures is given in [13]. However, we shall see that, for structures under impact loads, the scaling laws may become, so to say, distorted. If this is the case, test results on models cannot be traced back reliably to the prototype, loosing the advantage of the approach.

Many authors have investigated the problem of scaling impacted structures, [3], [4], [7], [9], [10],[12], [16], [19]. The Authors of paper [8] have highlighted some important issues of the problem by investigating, a beam under transverse impact using a numerical and an experimental technique. Dimensionless quantities related to impact structures have been also suggested, like the Johnson's damage number, D_n, which has been applied to the dynamic plastic response of beams and plates made of rigid-perfectly plastic materials.

Received 22 December 2003; accepted for publication 3 March 2004

R. E. Oshiro, M. Alves (✉)
Group of Solid Mechanics and Structural Impact – Department of Mechatronics and Mechanical Systems Engineering – University of São Paulo – São Paulo – 05508-900 – Brazil
All correspondence to be addressed to Dr. M. Alves
e-mail: maralves@usp.br

Zhao (1998) improved this number by including in [21] geometrical effects, and named it response number, R_n. He applied this number to express in a dimensionless form the response of simple impacted structures. Li and Jones critically discussed these numbers in [15], expanding them to include effects as strain hardening, strain rate, temperature and transverse shear loads. Papers [11] and [17] have shown the importance of the response number by applying it to the analysis of plates.

If we define a scaling factor as

$$\beta = \frac{l}{L} \quad , \tag{1}$$

where l and L correspond to the model and the prototype dimensions, respectively, we are able to relate some given variables of the model and prototype. For instance, the mass of a model should be β^3 times the mass of a prototype. This is achieved by applying simple dimensional analysis, as detailed in [3], [13]. Table 1 lists the relations between certain variables of interest in structures.

As previously indicated, structures under impact may not obey the usual scaling laws given in Table 1, and many factors can contribute to it, e.g. gravity, strain rate, inertia effects and fracture. This was found in the work [4] which was studying experimentally two different kinds of welded steel plate structures and showing the non-scalability of the final deformed configuration for the various impacted models, Fig. 1.

One reason for the experimental dimensionless data in Fig. 1 to depart from the expected scalability can be attributed to strain-rate effects and Table 1 helps to clarify the point. Suppose a material constitutive law is given by

$$\sigma_d = f(\dot{\varepsilon}) \quad ,$$

where σ_d and $\dot{\varepsilon}$ are the dynamic flow stress and strain rate, respectively. If a structure made from this material were to be scaled by β, we would obtain, from the strain-rate scaling factor in Table 1,

$$\sigma_d = f(\dot{\varepsilon}/\beta) \quad ,$$

which would contradict the same Table 1, since the stress scaling factor must be 1 for perfect similarity.

The fact that strain-rate effects are not prone to scaling is a major obstacle for the use of scaled structures under impact loads.

It is opportune to observe that, despite all the effort in the field, so far, it seems that no solution has been presented which could guarantee that model and prototype dynamically loaded and made from strain-rate sensitive materials can be scaled. This is a strong impediment for impact tests of scaled models. Accordingly, this paper presents a robust correction procedure which allows strain-rate sensitive model and prototype to behave strictly in a way that their final configuration are scaled. This is done by properly changing the initial impact velocity in a scaled impact test. The technique, explained in Sec. 2, is applied to three analytical models in Sec. 3, and discussed in Sec. 4.

2
Correction procedure

As indicated, strain-rate sensitive structures cannot be scaled by the usual technique. To overcome this shortcoming we develop in the sequence a non-direct similitude technique, also used in [8]. Differently from these authors, we apply our analysis only to the scaled structure

Table 1. Relationships between the model and the prototype

variable	scaling factor	variable	scaling factor	variable	scaling factor
length (L)	β	time (t)	β	strain (ε)	1
mass (G)	β^3	velocity (V)	1	acceleration (A)	$1/\beta$
stress (σ)	1	displacement (δ)	β	strain rate ($\dot{\varepsilon}$)	$1/\beta$

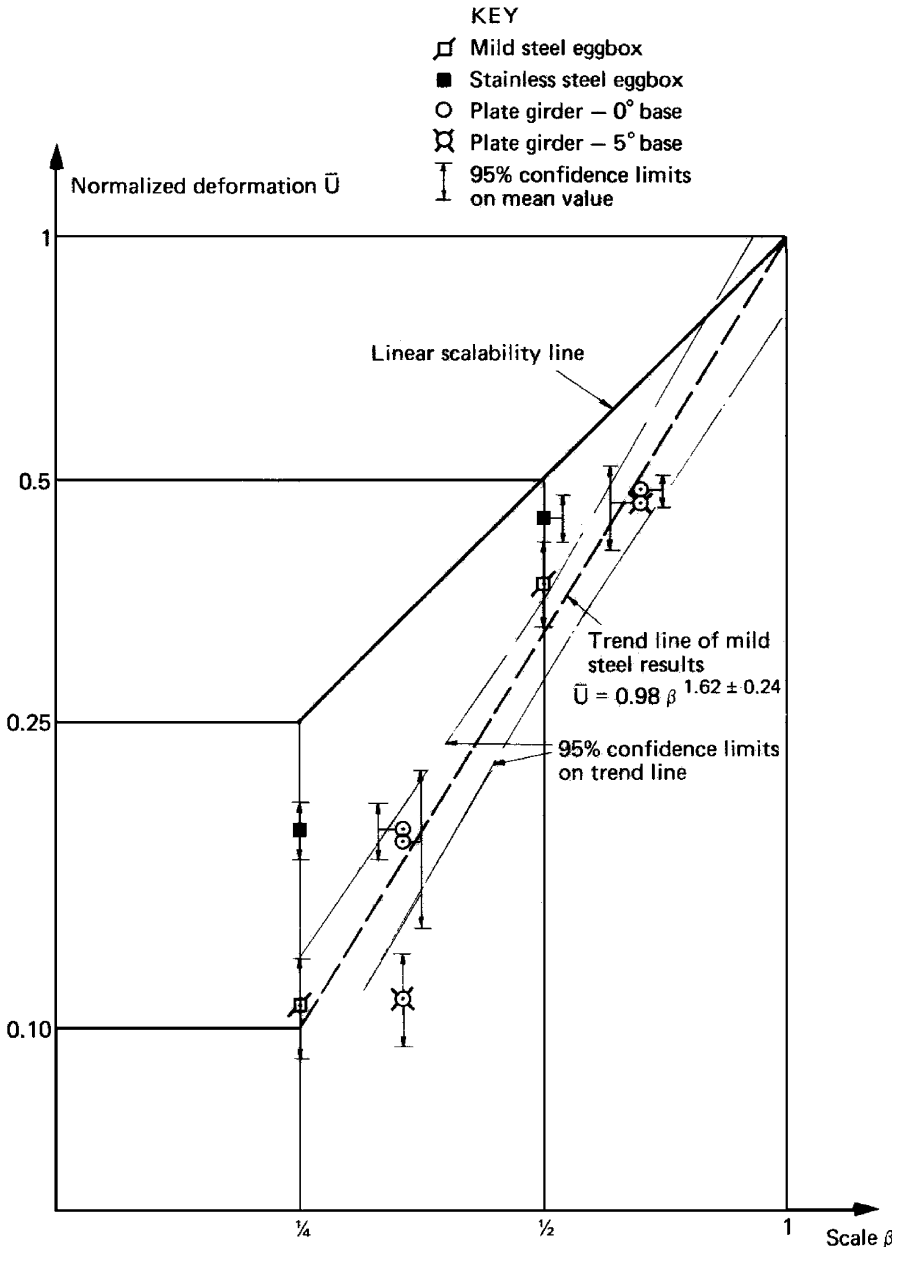

Fig. 1. Experimental dimensionless displacement of the prototype and various scaled models subjected to impact loads [4]

and from its response we are able to estimate the prototype behavior. The basic idea we pursue here is to change in a rational way the ratio between the impact velocity of the model and prototype and by so proceeding, both the model and the prototype reach the same final scaled configuration.

An important aspect is the use of a new set of dimensionless numbers based on the impact mass, G, the initial impact velocity, V_0, and on the dynamic yielding stress, σ_d. This new basis is an alternative to the traditional approach which uses the MLT (mass, length, time) basis. We then arrive at the reduced dimensional matrix in Table 2, formed by expressing the relevant variables of an impact phenomenon, i.e. acceleration, A, time, T, displacement, δ, strain rate, $\dot{\varepsilon}$, and stress, σ as functions of the new basis V_0, σ_d and G.

Standard procedures in dimensional analysis allows to generate the following dimensionless Π-terms:

Table 2. Reduced dimensional matrix

		variables				
		A	T	δ	$\dot{\varepsilon}$	σ
basis	V_0	4/3	−1/3	2/3	1/3	0
	σ_d	1/3	−1/3	−1/3	1/3	1
	G	−1/3	1/3	1/3	−1/3	0

$$\underbrace{\left[\frac{A^3 G}{V_0^4 \sigma_d}\right]}_{\Pi_1}, \underbrace{\left[\frac{T^3 \sigma_d V_0}{G}\right]}_{\Pi_2}, \underbrace{\left[\frac{\delta^3 \sigma_d}{G V_0^2}\right]}_{\Pi_3}, \underbrace{\left[\dot{\varepsilon}\left(\frac{G}{\sigma_d V_0}\right)^{1/3}\right]}_{\Pi_4}, \underbrace{\left[\frac{\sigma}{\sigma_d}\right]}_{\Pi_5} \quad , \tag{2}$$

for later use.

The fundamental problem we have set to solve is the non-scalability of impacted structures due to strain-rate effects which, in turn, affect the flow stress. A scaling factor for the dynamic stress is defined as

$$\beta_{\sigma_d} = \frac{\sigma_{d_m}}{\sigma_{d_p}} = \frac{f(\dot{\varepsilon}_m)}{f(\dot{\varepsilon}_p)} \quad , \tag{3}$$

where the indices m and p stand for model and prototype and f is a generic function given by the material constitutive law.

We seek to find the correct strain rate for the model, $\dot{\varepsilon}_m^c$, such that

$$\beta_{\sigma_d} = \frac{f(\dot{\varepsilon}_m^c)}{f(\dot{\varepsilon}_p)} \quad . \tag{4}$$

Assuming that $\dot{\varepsilon} \propto V_0/L$, we can write

$$\frac{\dot{\varepsilon}_m^c}{\dot{\varepsilon}_m^{nc}} = \frac{\beta_{V_0} V_0/L}{V_0/L} = \beta_{V_0} \quad , \tag{5}$$

where nc stands for non-correct and

$$\beta_{V_0} = \frac{V_{0_m}}{V_{0_p}} \tag{6}$$

is the scaling factor for the impact velocity.

Obviously that β_{V_0} should be 1 for a non-distorted model; however, for a strain-rate sensitive material we need to find an initial impact velocity for the model such that model and prototype are scaled. This can be achieved by using the dimensionless number Π_3 from Eq. (2), leading to

$$\frac{\Pi_{3_m}}{\Pi_{3_p}} = \frac{\beta_\delta^3 \beta_{\sigma_d}}{\beta_G \beta_{V_0}^2} = \frac{\beta^3 \beta_{\sigma_d}}{\beta^3 \beta_{V_0}^2} = 1 \quad , \tag{7}$$

and so

$$\beta_{\sigma_d} = \beta_{V_0}^2 \quad . \tag{8}$$

Now,

$$\beta_{\dot{\varepsilon}} = \frac{\dot{\varepsilon}_m}{\dot{\varepsilon}_p} \quad , \tag{9}$$

but we rewrite it as

$$\beta_{\dot{\varepsilon}} = \frac{\dot{\varepsilon}_m^c}{\dot{\varepsilon}_p} \quad , \tag{10}$$

since we are seeking for the correct strain rate. Furthermore,

$$\beta_{\dot{\varepsilon}} = \frac{\beta_{V_0}}{\beta} \tag{11}$$

can be obtained from $\Pi_{4_m}/\Pi_{4_p} = 1$. Therefore, from Eqs. (5) and (10), it follows that

$$\beta_{\dot{\varepsilon}} = \frac{\beta_{V_0}\dot{\varepsilon}_m^{nc}}{\dot{\varepsilon}_p} \quad . \tag{12}$$

Finally, using Eq. (11) and (12) it can be shown that

$$\dot{\varepsilon}_p = \beta\dot{\varepsilon}_m^{nc} \quad , \tag{13}$$

which allows the calculation of the new (corrected) β_{V_0}

$$\beta_{V_0} = \sqrt{\beta_{\sigma_d}} = \sqrt{\frac{\sigma_{d_m}}{\sigma_{d_p}}} = \sqrt{\frac{f(\dot{\varepsilon}_m^c)}{f(\dot{\varepsilon}_p)}} = \sqrt{\frac{f(\beta_{V_0}\dot{\varepsilon}_m^{nc})}{f(\beta\dot{\varepsilon}_m^{nc})}} \quad , \tag{14}$$

when bearing in mind Eqs. (5), (8) and (13).

Equation (14) is the key for correcting the distortion of a model subject to an impact load. It requires to know the strain rate in the non-corrected model, $\dot{\varepsilon}_m^{nc}$, and the dimensional scaling factor, β, to be applied in the constitutive model, so that the stress levels can be calculated. A straightforward recursive procedure is then used to extract β_{V_0}, and so the corrected impact velocity which, when applied to the model, will make it to behave as with no distortion. Observe that the approach here only sets a way to correct the initial impact velocity, so that the strain rate and the dynamic flow stress are properly altered. The particular form of the constitutive model, as described by the function f, is not relevant in the approach here developed.

It is opportune to observe that other variables are of interest in an impact event. We see from Table 1 that time is scaled by a factor β. However, due to the inherited distortion of the model, time needs to be corrected. To do so, we can use, for instance, the dimensionless numbers Π_2, such that

$$\frac{\Pi_{2_m}}{\Pi_{2_p}} = \frac{\beta_T^3\beta_{\sigma_d}\beta_{V_0}}{\beta_G} = 1 \quad , \tag{15}$$

which results in

$$\beta_T = \frac{\beta}{\beta_{V_0}} \quad . \tag{16}$$

Observe that in both Eqs. (7) and (16), $\beta_G = \beta^3$ because we deliberately enforced the standard scaling law for mass. By manipulating the various dimensionless numbers formed using the new basis, Eq. (2), it is straightforward to show that the acceleration scales according to

$$\beta_A = \frac{\beta_{V_0}^2}{\beta} \quad . \tag{17}$$

The correction procedure here suggested can be summarized in the following basic steps:

(1) simulate the model scaled by β
(2) obtain the non-corrected strain rate, $\dot{\varepsilon}^{nc}$

(3) calculate β_{V_0} from Eq. (14)
(4) calculate the new impact velocity from β_{V_0} and the original impact velocity
(5) perform step 1 but with the new corrected velocity

By applying this procedure, the final geometry of the model the and the prototype will be scaled by the desired factor β. Observe that variables like acceleration, time, strain rate and stress do not scale according to Table 2. Nevertheless, they can equally be predicted with the help of Eq. (8), for stress, Eqs. (11) for strain rate, Eq. (16) for time and Eq. (17) for acceleration. Note that if $\beta_{V_0} = 1$, all the equations presented here reduce to what we could call linear scaling laws.

3
Correcting some distorted models

In this section, we apply the correction procedure described before to two basic structures subject to dynamic impact loads sufficiently intense to cause material plastic flow but not failure. The structures under analysis were chosen in order to highlight some peculiar features. Accordingly, a double plate structure under axial impact load was elected because it exhibits two phases of motion, with compression and bending in the presence of buckling. We also chose a clamped beam subject to an impulsive velocity which undergoes finite displacements. These models have all theoretical solutions, whose responses do not scale when they are based on a strain-rate sensitive material. It is shown that the technique here suggested allows the response of these structures to be properly scaled.

3.1
Plate under axial impact

Consider two plates clamped together at the base and at the top as shown in Fig. 2. The plates were pre-bent by a small initial rotation and axially impacted by a mass, G, travelling with an initial velocity V_0. This configuration was studied experimentally in [5] and [18]. The structure typically responds with an initial peak load followed by a stiff decreasing load and it has been classified as type II structure. To the present context, it is relevant to observe that structures of type II are very sensitive to strain-rate effects and broadly it comprises of plates loaded in-plane.

3.1.1
Basic equations

The model in Fig. 2 has two phases of motion which were described in [18] and [20]. The initial stage is dominated by axial compression, q, of the plates and it is ruled by

$$V_0 - \frac{S\sigma_d}{G}t = 2\left(\frac{12\sigma_d S}{ml}\right)^{1/2}\frac{w_0^2}{l}\sinh\left[2\left(\frac{12\sigma_d S}{ml}\right)^{1/2}t\right] + \dot{q} \ . \tag{18}$$

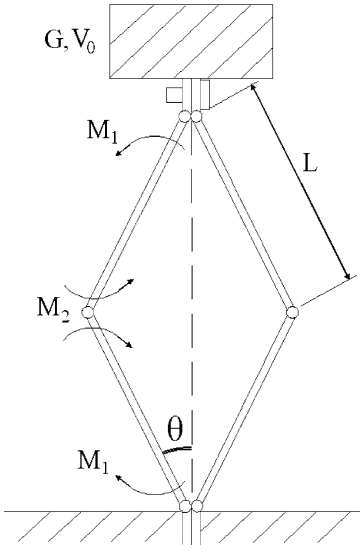

Fig. 2. A two-plate structure under axial impact

This stage ends at $t = \tau_1$, obtained by solving

$$V_0 - \frac{S\sigma_d}{G}\tau_1 = 2\sqrt{\frac{12S\sigma_d}{ml}}\frac{w_0^2}{l}\sinh\left(2\sqrt{\frac{12S\sigma_d}{ml}}\tau_1\right) \ , \tag{19}$$

where S is the cross section of the bar, $l = 2L$, m is the mass of the bars and w_0 is the horizontal displacement at the center of the bars corresponding to the initial rotation, θ_0, σ_d is the dynamic flow stress obtained using the Cowper–Symmonds equation, [1]

$$\sigma_d = \sigma_0\left\{1 + \left(\frac{\dot{\varepsilon}}{D}\right)^{1/p}\right\} \ , \tag{20}$$

where D and p are material constants and σ_0 is the quasi-static flow stress.

The final rotation and angular velocity at this first phase of motion are given by

$$\theta_1 = \frac{2}{l}w_0\cosh\left\{\sqrt{\frac{12S\sigma_d}{ml}}\tau_1\right\} \tag{21}$$

and

$$\dot{\theta}_1 = \frac{2}{l}w_0\sqrt{\frac{12S\sigma_d}{ml}}\sinh\left\{\sqrt{\frac{12S\sigma_d}{ml}}\tau_1\right\} \ , \tag{22}$$

which are used as initial conditions for the second (bending) phase of motion ruled by

$$\ddot{\theta} + \frac{L^2(m+G)\sin\theta\cos\theta\dot{\theta}^2 + M_1 + M_2}{L^2\left[\frac{m}{3} + (m+G)\sin^2\theta\right]} = 0 \ , \tag{23}$$

possible to be solved numerically when adopting

$$M_1 = \left[\left(\frac{\dot{\theta}}{8D}\right)^{1/p}\frac{2p}{2p+1} + 1\right]M_0 \tag{24}$$

and

$$M_2 = \left[\left(\frac{\dot{\theta}}{4D}\right)^{1/p}\frac{2p}{2p+1} + 1\right]M_0 \quad , \tag{25}$$

where $M_0 = \sigma_0 bh^2/4$, b and h are the plate width and thickness respectively. A hinge length of $4h$ was adopted, [18].

A simple analysis of the above governing equations shows that the non-scalability of the model is solely due to the constitutive equation via the strain-rate effects, since when scaling the moments by a factor β it results in

$$M_1 = \left[\left(\frac{\beta_{V_0}\dot{\theta}}{8\beta D}\right)^{1/p}\frac{2p}{2p+1} + 1\right]M_0 \tag{26}$$

and

$$M_2 = \left[\left(\frac{\beta_{V_0}\dot{\theta}}{4\beta D}\right)^{1/p}\frac{2p}{2p+1} + 1\right]M_0 \ . \tag{27}$$

Obviously, that the model can become strongly distorted according to the material parameters D and p, as shown next.

3.1.2
Correction procedure

The equations of motion developed in the previous section for the in-plane plate impact were solved numerically for two different materials, mild steel and aluminum alloy. Since the mild steel is quite strain-rate sensitive, the distortion in a scaled model should be more evident than in the less strain-rate sensitive aluminium alloy.

To obtain the correction factor, the equation of motions (18) and (23) are solved initially with no correction whatsoever, i.e. $\beta_{V_0} = 1$. The value of $\dot{\theta}^{nc}$ at the end of the motion is then used in Eq. (14), which becomes

$$\beta_{V_0} = \left[\frac{\left(\frac{\beta_{V_0} \dot{\theta}_m^{nc}}{4D} \right)^{1/p} \frac{2p}{2p+1} + 1}{\left(\frac{\beta \dot{\theta}_m^{nc}}{4D} \right)^{1/p} \frac{2p}{2p+1} + 1} \right]^{1/2}, \tag{28}$$

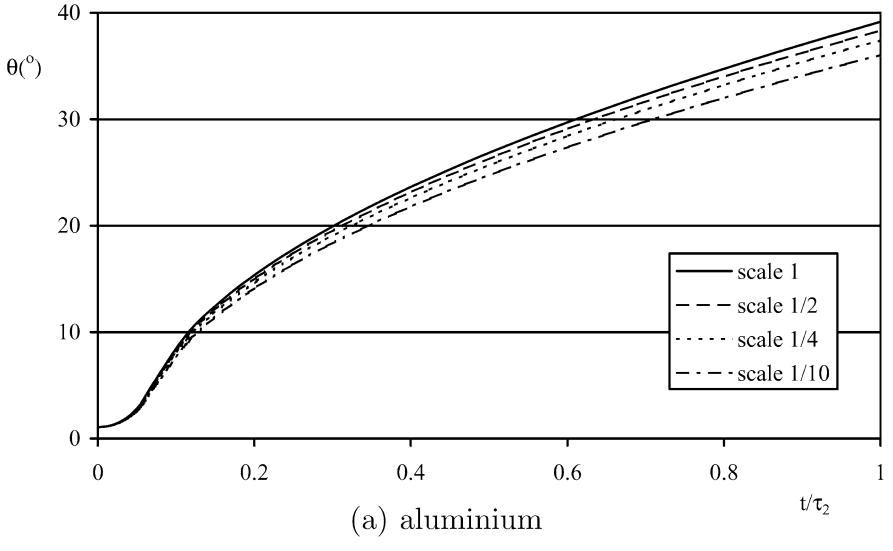

(a) aluminium

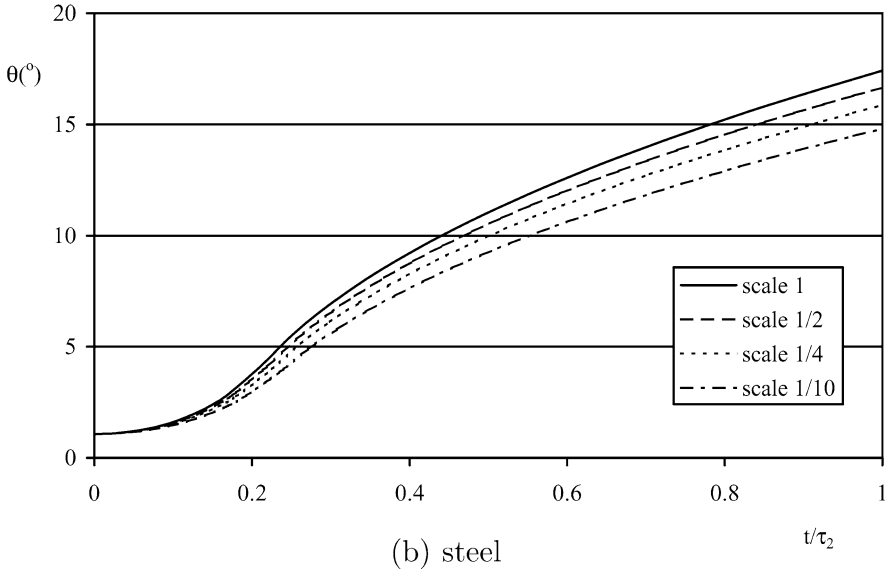

(b) steel

Fig. 3. Evolution of the plate rotation for different scaling factors when no correction for distortion is applied

for the present case. This allows the calculation of β_{V_0}, to be used in all the scaled equations of motion and in the dynamic flow stress presented in the (scaled) initial conditions for the second phase of motion, Eqs. (21) and (22).

3.1.3 Results

The evolution of the rotation angle, θ, is shown in Fig. 3 for different scaling factors, both for aluminium and steel plates described in Table 3. It is evident that the angular motion is quite sensitive to the scaling factor, even for the aluminium alloy.

Figure 3 shows clearly the non-scalability and this effect is attributed to the influence of the strain rate on the flow stress. Note that the decrease of the scaling factor means larger strain rates with the consequent increase of the material flow stress and the decrease of the rotation. Relative to the prototype, the observed deviations of the non-corrected scaled models are listed in Table 4 (aluminium) and Table 5 (steel) for various scaling factors and variables of the phenomenon at the end of the motion.

Our initial claim that it is possible to correct a distorted model is now demonstrated when comparing the errors in these tables, where it is evident that the correction procedure significantly decreases the errors.

Visually, the decrease of the errors can be better appreciated in Fig. 4, which shows the evolution of the rotation angle of the plate with time for various scaling factors. Note that, even for steel plates, the error is quite small and acceptable.

Table 3. Geometry and material properties of the plates

geometry	mild steel	aluminium
$L = 25$mm	$\rho = 7800$kg/m^3	$\rho = 2700$kg/m^3
$h = 1.6$mm	$\sigma_0 = 235$Mpa	$\sigma_0 = 100$Mpa
$b = 5.0$mm	$p = 5$	$p = 4$
$\theta_0 = 1.07^\circ$	$D = 40$/s	$D = 6500$/s
G (kg)	6.41	6.41

Table 4. Results at the end of the motion for corrected, ^{c}, and non-corrected, ^{nc}, models made of aluminium. Errors are absolute and relative to the prototype ($\beta = 1$)

Variable	$\beta = 1$	$\beta = 1/2$	$\beta = 1/4$	$\beta = 1/10$
β_{V_0}	1.00	1.02	1.04	1.08
$\theta^c(^\circ)$	39.18	39.19	39.21	39.25
$\theta^{nc}(^\circ)$	39.15	38.33	37.41	36.04
error$^c(\%)$	0.00	0.03	0.08	0.18
error$^{nc}(\%)$	0.08	2.17	4.52	8.01
τ_1^c(ms)	1.97	1.97	1.97	1.97
τ_1^{nc}(ms)	1.97	1.98	1.89	1.77
error$^c(\%)$	0.00	0.00	0.00	0.00
error$^{nc}(\%)$	0.00	0.51	4.06	10.15
A^c(m/s^2)	3138.00	3137.00	3136.00	3131.00
A^{nc}(m/s^2)	3137.65	3261.80	3410.80	3654.46
error$^c(\%)$	0.00	0.03	0.06	0.22
error$^{nc}(\%)$	0.01	3.95	8.69	16.46
$\dot{\varepsilon}^c$(1/s)	181.43	181.37	181.23	180.90
$\dot{\varepsilon}^{nc}$(1/s)	181.43	184.11	187.50	192.94
error$^c(\%)$	0.00	0.03	0.11	0.29
error$^{nc}(\%)$	0.00	1.48	3.35	6.34
σ^c(MPa)	125.69	125.67	125.62	125.44
σ^{nc}(MPa)	125.69	130.66	136.63	146.39
error$^c(\%)$	0.00	0.02	0.06	0.20
error$^{nc}(\%)$	0.00	3.95	8.70	16.47

Table 5. Results at the end of the motion for corrected, ^{c}, and non-corrected, ^{nc}, models made of steel. Errors are absolute and relative to the prototype ($\beta = 1$)

variable	$\beta = 1$	$\beta = 1/2$	$\beta = 1/4$	$\beta = 1/10$
β_{V_0}	1.00	1.04	1.08	1.15
$\theta^c(^\circ)$	17.45	17.46	17.47	17.50
$\theta^{nc}(^\circ)$	17.42	16.66	15.87	14.81
error^c(%)	0.00	0.06	0.11	0.29
error^{nc}(%)	0.17	4.53	9.05	15.13
τ_1^c (ms)	0.51	0.51	0.51	0.51
τ_1^{nc} (ms)	0.51	0.49	0.45	0.40
error^c(%)	0.00	0.20	0.20	0.39
error^{nc}(%)	0.00	3.73	11.57	21.37
A^c (m/s^2)	12086.00	12082.00	12071.00	12044.00
A^{nc} (m/s^2)	12086.20	13059.53	14195.19	15985.22
error^c(%)	0.00	0.03	0.12	0.35
error^{nc}(%)	0.00	8.06	17.45	32.26
$\dot{\varepsilon}^c$ (1/s)	345.25	345.06	344.78	344.17
$\dot{\varepsilon}^{nc}$ (1/s)	345.25	357.12	371.62	393.46
error^c(%)	0.00	0.06	0.14	0.31
error^{nc}(%)	0.00	3.44	7.64	13.96
σ^c (MPa)	484.77	484.01	483.57	482.47
σ^{nc} (MPa)	484.16	523.15	568.64	640.35
error^c(%)	0.00	0.16	0.25	0.47
error^{nc}(%)	0.13	7.92	17.30	32.09

3.2
Clamped beam subject to a uniformly distributed velocity pulse

We analyse now another category of structures, namely beams under transverse impact loading, aiming to show that the approach here developed is quite robust, regardless of the type of structure or loading.

The problem is of a beam loaded with an initial impact velocity throughout all its span, Fig. 5. Different phases of motion exist in this problem, as detailed in [13]. Here of interest is the final maximum displacement achieved by the prototype and the model.

3.2.1
Basic equations

The final displacement for this class of beams, W_f, can be obtained by applying the following equation:

$$\frac{W_f}{H} = \frac{1}{2}\left\{\left(1 + \frac{3\lambda}{4}\right)^{1/2} - 1\right\}, \tag{29}$$

where H is the beam depth and

$$\lambda = \frac{4\rho V_0^2 L^2}{\sigma_0 H^2} \tag{30}$$

is a dimensionless impact energy. It can be shown [2], that Eq. (29) becomes

$$\frac{W_f}{H} = \frac{1}{2}\left[\left(1 + 3\frac{\rho V_0 L^2}{n\sigma_0 h^2}\right)^{1/2} - 1\right] \tag{31}$$

when strain-rate effects are cared for using the Cowper–Symmonds equations, with

$$n = \frac{\sigma_d}{\sigma_0} = 1 + \left(\frac{V_0 W_f}{3\sqrt{2}DL^2}\right)^{1/p} \tag{32}$$

and the average strain rate

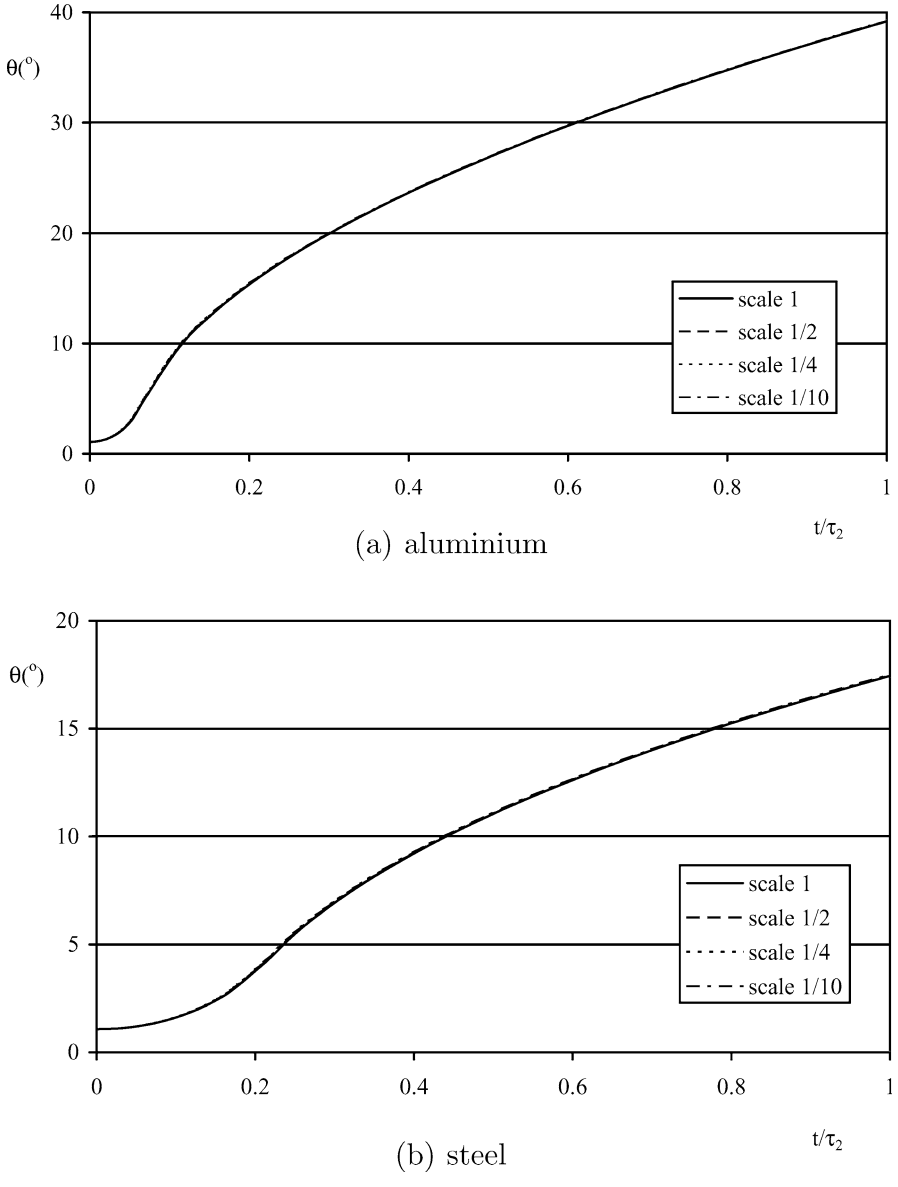

Fig. 4. Evolution of the plate rotation for different scaling factors with correction for distortion applied

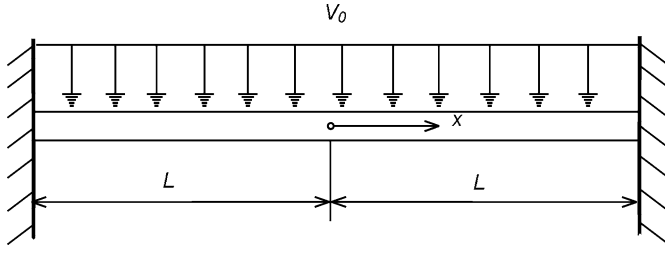

Fig. 5. A clamped beam under transverse blast load

$$\dot{\varepsilon} = \frac{V_0 W_f}{3\sqrt{2}L^2} \quad . \tag{33}$$

Observe that Eq. (31) takes finite displacements into account as well as strain-rate effects in the material response. Also, scaled structures would have the same scaled final displacement according to Eq. (31) if it were not for the strain-rate sensitivity factor, n, which, when scaled, gives

$$n = 1 + \left(\frac{V_0 W_f}{3\sqrt{2} D \beta L^2} \right)^{1/p} \quad , \tag{34}$$

where it can be seen that the scale factor, β, cannot be eliminated.

3.2.2 Correction procedure and results

The correction procedure to be applied is rather simple and it consists in obtaining the new scaling factor β_{V_0} from Eq. (14), which yields

$$\beta_{V_0} = \left[\frac{1 + \left(\frac{\beta_{V_0} \dot{\varepsilon}_m^{nc}}{D} \right)^{1/p}}{1 + \left(\frac{\beta \dot{\varepsilon}_m^{nc}}{D} \right)^{1/p}} \right]^{1/2} \quad . \tag{35}$$

Now, the non-correct strain rate for the model is

$$\dot{\varepsilon}_m^{nc} = \frac{V_0 W_{f_m}^{nc}}{3\sqrt{2} L_m^2} \quad , \tag{36}$$

finally giving

$$\beta_{V_0} = \sqrt{\frac{1 + \left(\frac{\beta_{V_0} V_0 W_{fm}^{nc}}{3\sqrt{2} D L_m^2} \right)^{1/p}}{1 + \left(\frac{\beta V_0 W_{fm}^{nc}}{3\sqrt{2} D L_m^2} \right)^{1/p}}} \quad , \tag{37}$$

which can be solved numerically with regard to β_{V_0}.

We applied the model to a mild steel beam with $\sigma_0 = 210.3$ MPa, $\rho = 7829$ kg/m^3, $H = 2.3$mm and $L = 63.7$mm, with the Cowper-Symmonds parameters of $p = 5$ and $D = 40.5$ /s. The impulsive velocity is $V_0 = 50$m/s and Table 6 lists the final displacement and errors for both the corrected and non-corrected models and different scaling factors. We deliberately used a mild steel for its known strain-rate sensitivity, which is the only aspect in this problem causing distortion of the scaling laws, as already detailed.

4 Discussion

The possibility of working with strain-rate sensitive scaled structures has been severely limited when they are loaded dynamically in a way to exhibit plastic deformation. The fact that the material increases its resistance as the impact load is applied makes the scaling laws to be distorted. This can easily be seen by examining the Cowper-Symmonds constitutive law, Eq. (20). The model to prototype dynamic flow stress ratio is given by, [13]

$$\frac{\sigma_{d_m}}{\sigma_{d_p}} = \frac{1 + \left(\frac{1}{\beta} \right)^{1/p}}{2} \quad , \tag{38}$$

Table 6. Results for the final corrected, ^{c}, and non-corrected, ^{nc}, displacement of mild steel beams impulsively loaded with $V_0 = 50$m/s. Errors are absolute and relative to the prototype ($\beta = 1$)

β	W_f/H^{nc}	error^{nc}(%)	β_{V_0}	W_f/H^c	error^c(%)
1	4.66	0.00	1.00	4.66	0.00
1/2	4.50	3.57	1.04	4.66	0.01
1/4	4.33	7.24	1.08	4.66	0.06
1/10	4.10	12.18	1.14	4.66	0.16
1/20	3.92	15.96	1.19	4.65	0.28

when the strain rate equals the material parameter D. For $q = 5$, Fig. 6 shows how relevant is the departure of the stress in the model from the prototype, suggesting that models with large scaling factors cannot possibly be tested under impact loads causing strain rates of the order of the constant D.

It seems that so far there is no technique available to properly correct a scaled model under impact loads. The present work explores this problem by suggesting a robust, simple and accurate technique, so that any sought variable can be scaled. This opens the possibility for impact tests on scaled structures.

The technique was applied to structures of type I and II with the sole purpose to demonstrate that structures with radically different behaviour and undergoing different phases of motion can be scaled with a minimum error.

It is important to point out that the chosen strain rate used in the correction procedure was the one at the final phase of motion for the in-plane impacted plate and a constant value throughout all the motion for the beam. This is to say that we cannot correct all stages at same time. Nevertheless, the errors were always quite small, confirming that the technique is quite accurate.

It is implicit in all the above calculations that the approximation

$$\dot{\varepsilon} \propto \frac{V_0}{L} \tag{39}$$

holds.

However, this relationship might be too simple to describe the strain rate in some structures. The studied models exhibited a good agreement partially due to the fact that the actual strain rates are closer to the relation in Eq. (39), as indicated in Fig. 7 for the plates under axial impact.

The work from [8] uses a non-direct similitude approach but it differs substantially from what we suggest here. One important point is that the technique presented in [8] needs to perform a test on the prototype in order to infer the behaviour of a scaled model. This is not desirable, especially in the context of analysis of large impacted structures.

Paper [6] has suggested a correction procedure for distorted models in which the initial impact velocity is scaled by β. Although this breaks the natural scaling laws, it implies that the strain rate in both model and prototype are the same. This leads to equal stresses in the model and prototype, since σ_d does not change with β, as it can be seen from

$$\sigma_d = \sigma_0 \left[1 + \frac{\beta V_0}{D\beta l}\right]^{1/p} = \sigma_0 \left[1 + \frac{V_0}{Dl}\right]^{1/p} . \tag{40}$$

However, in order to scale the input energy, it is necessary to scale the drop mass by β and not by β^3, as usual. If this scheme is adopted for the axial impact of a plate made of mild steel and with the same geometry and initial conditions as before, the results are quite poor, as it can be seen in Fig. 8, which can be compared with Fig. 4(b).

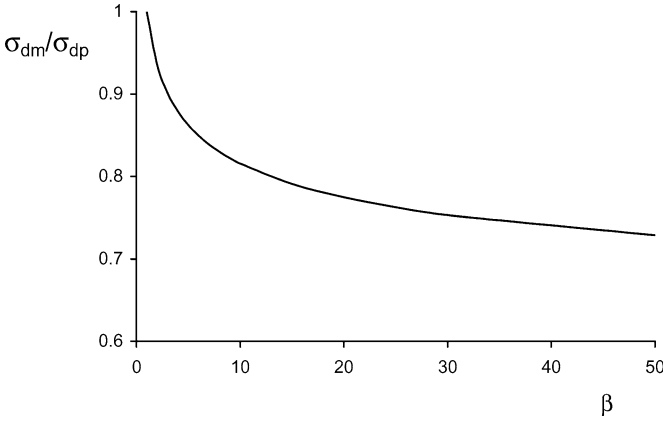

Fig. 6. Influence of the scaling factor on the flow stress at $\dot{\varepsilon} = D$ and $q = 5$

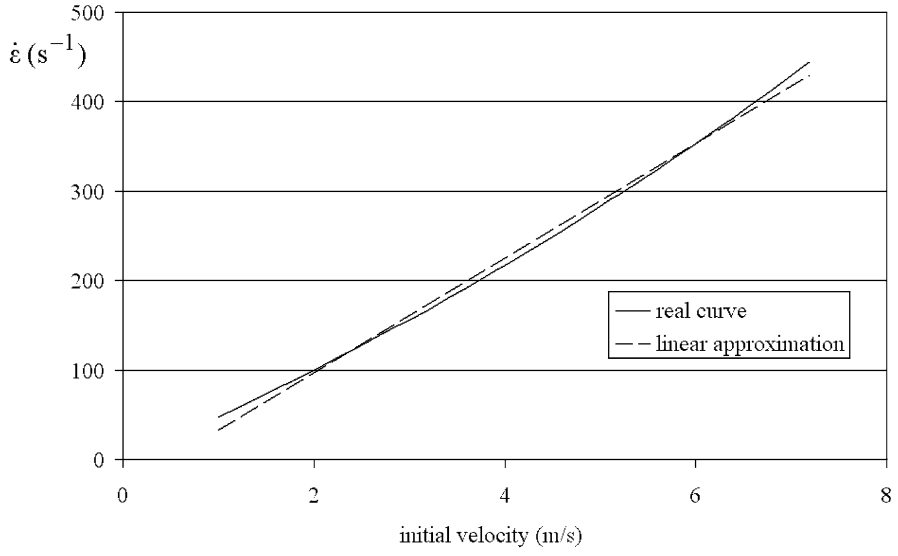

(a) axial plate impact

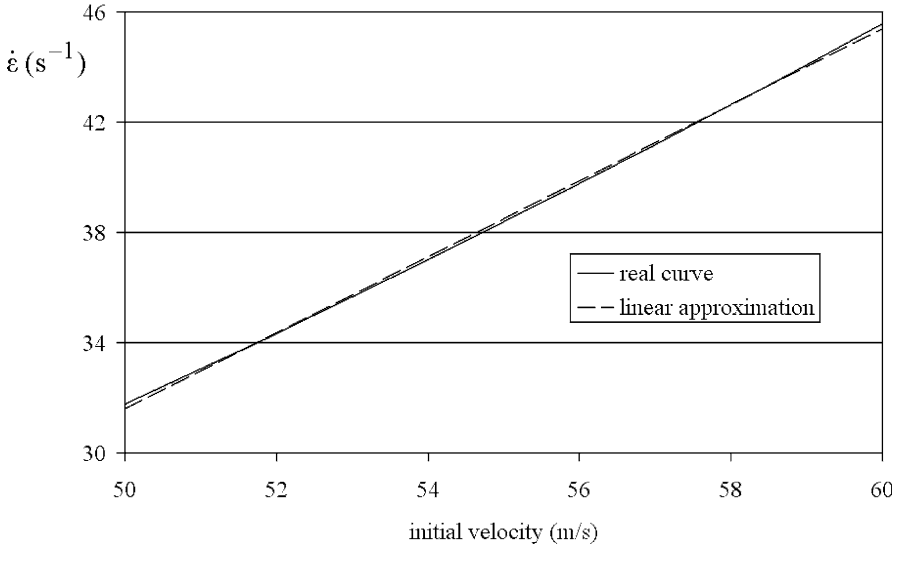

(b) blast load

Fig. 7. Actual strain rate in the plate problem and as given by Eq. (39)

One of the reasons for this strong distortion is that the time for completion of the first phase of motion becomes rather distorted and not linearly proportional to β, as it should be the case for the linear scaling laws (s. Table 1) when no strain rate effect is considered.

5 Conclusions

A technique has been described which allows for the correction of distorted models in a way that the final configurations of the model and prototype are properly scaled. The idea is to alter the impact velocity which in turn alters the strain rate. It is the strain rate the variable responsible for the non-scalability of the structural models studied here.

The procedure yields information for the calculation of the corrected velocity factor which is subsequently used to calculate the new velocity. By applying this later velocity to the scaled model, the scalability of the structure is guaranteed within a very small error.

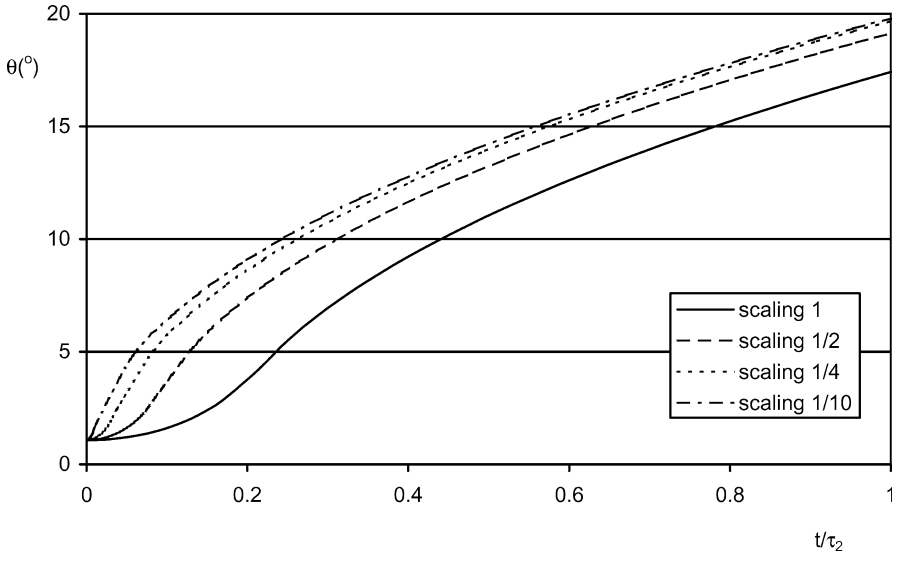

Fig. 8. Evolution of the mild steel plate rotation for different scaling factors when adopting the correction given in [6]

Moreover, the results give the values of time, acceleration, strain rate and stress for the scaled structure, such that it is now possible to work with scaling models made from strain-rate sensitive materials.

In this work, only strain rate effects have been studied. It can be concluded that the important problem of distortion of scaling models due to these effects has been solved by the simple, robust and accurate method presented in the paper.

References

1. **Alves, M.:** Material constitutive law for large strains and strain rates. J Eng Mech 126(2) (2000) 215–218
2. **Alves, M.; Jones, N.:** Impact failure of beams using damage mechanics: Part I – Analtical model. Int J Impact Eng 27(8) (2002) 837–861
3. **Baker, W.; Westine, P.; Dodge, F.:** Similarity methods in engineering dynamics. Elsevier
4. **Booth, E.; Collier, D.; Miles, J.:** Impact scalability of plated steel structures. In: Jones,N., Wierzbicki, T. (eds.) Structural crashworthiness. Butterworths, London (1983) pp. 136–174
5. **Calladine, C.; English, R.:** Strain rate and inertial effects in the collapse oftwo typesof energy-absorbing structure. Int J Mech Sci 26 (1986) 689–701
6. **Calladine, R.:** An investigation of impact scaling theory (appendix). In: Jones, N., Wierzbicki, T. (eds.), Structural crashworthiness. Butterworths, London (1983) pp. 169–174
7. **Carpinteri, A.:** Size-scale effects in the failure mechanisms of materials and structures. E & FN Spon, London (1996)
8. **Drazetic, P.; Ravalard, Y.; Dacheux, F.; Marguet, B.:** Applying non-direct similitude technique to the dynamic bending collapse of rectangular section tubes. Int j Impact Eng 15(6) (1994) 797–814
9. **Duffey, T.:** Scaling laws for fuel capsules subjected to blast, impact and thermal loading. In: Proc of the Intersociety Energy Conversion Eng Conference. SAE, (1971) pp. 775–786
10. **Duffey, T.; Cheresh, M.; Sutherland, S.:** Experimental veification of scaling laws for punch-impact-loaded structures. Int J Impact Eng 2(1) (1984) 103–117
11. **Hu, Y.:** Application of response number for dynamic plastic response of plates subjected to impulsive loading. Int J Pressure Vessels Piping 77 (2000) 711–714
12. **Jones, N.:** Scaling of inelastic structures loaded dynamically. In: Davies, G. (ed.), Structural impact and crashworthiness. Elsevier Appl Sci (1984) pp. 45–74
13. **Jones, N.:** Structural impact. Cambridge University Press, Cambridge (1989)
14. **Jones, N.; Jouri, W.; Birch, R.:** On the scaling of ship collision damage. In: Third Int Congress on Marine Technology. Athens, (1984) pp. 287–294
15. **Li, Q.; Jones, N.:** On dimensionless number for dynamic plastic respose of structural nembers. Arch Appl Mech 70 (2000) 245–254
16. **Nurick, G.; Martin, J.:** Deformation of thin plates subjected to impulsive loading - a review, Part II: Experimental studies. Int J Impact Eng 8 (1989) 171–186
17. **Shi, X.; Gao, Y.:** Generalization of response number for dynamic plastic response of shells subjected to impulsive loading. Int J Pressure Vessels Piping 78 (2001) 453–459
18. **Tam, L.; Calladine, C.:** Inertia and strain-rate effects in a simple plate-structure inder impact loading. Int J Impact Eng 11 (1991) 349–377

19. **Wen, H.; Jones, N.:** Experimental investigation of the scaling laws for metal plates struck by large masses. Int J Impact Eng 13(3) (1993) 485–505
20. **Zhang, T.; Yu, T.:** A note on a velocity sensitive energy-absorbing structure. Int J Impact Eng 8 (1989) 43–51
21. **Zhao, Y.:** Suggestion of a new dimensionless number for dynamic plastic respose of beams and plates. Arch Appl Mech 68 (1998) 524–538